Int J Adv Manuf Technol (2017) 91:2777–2786
DOI 10.1007/s00170-016-9913-5

ORIGINAL ARTICLE

Numerical study on the temperature field of underwater flux-cored wire arc cutting process

Jianxin Wang[1,2] · **Jiahui Shi**[1] · **Jiayou Wang**[1] · **Wenhang Li**[1,2] · **Chuan Liu**[1] · **Guoxiang Xu**[1] · **Sergii Yuri Maksimov**[3] · **Qing Zhu**[1]

Received: 17 August 2016 / Accepted: 18 December 2016 / Published online: 11 January 2017
© Springer-Verlag London 2017

Abstract The fast development of ocean engineering makes the underwater cutting more and more important. In present study, a special underwater wet cutting method, namely the underwater flux-cored wire arc cutting (FCAC) was introduced. The underwater cutting experiment was conducted using flux-cored wire cutting method, and experimental as well as numerical analysis was carried out to investigate the temperature field during underwater FCAC process. According to the mechanism of the underwater FCAC, double ellipsoid heat source model considering arc heat as well as chemical heat was introduced, and the boundary condition of pool boiling heat transfer was selected. The calculated thermal cycles during underwater FCAC process match well with those acquired by the experiment, which proves the model and boundary condition in this study to be applicable for underwater FCAC. It is found that the calculated $t_{8/5}$ value is shorter than 0.5 s, which is much shorter than the one of air-arc cutting process and the one of underwater welding process. In addition, the heat affected zone (HAZ) near the cut cavity is determined, which is expected to facilitate the further research on the cutting mechanism, as well as the optimization of cutting parameters.

✉ Jianxin Wang
Wangjx_just@126.com

[1] Jiangsu Provincial Key Lab of Advanced Welding Technology, Jiangsu University of Science and Technology, Zhenjiang 212003, China

[2] College of Material Science and Technology, Nanjing University of Aeronautics and Astronautics, Nanjing 210016, China

[3] E. O. Paton Electric Welding Institute, NASU, 11 Bozhenko Str., 03680, Kyiv 150, Ukraine

Keywords Underwater wet cutting · Flux-cored wire · Finite element method · Temperature field · Heat affected zone

1 Introduction

Underwater cutting is an important technique for both repair of marine pipelines and construction of marine structures. In addition, underwater cutting also plays a significant role in nuclear reactors disassemble, underwater repair of ship building and underwater salvage [1]. It has been acknowledged that the safe and efficient removal of base metal will undoubtedly require the development of specific underwater cutting [2, 3]. E. O. Paton electric welding institute has made a substantial contribution into the advancement of underwater wet welding & cutting technology, and invents flux-cored wire arc welding (FCAW) as well as flux-cored wire arc cutting (FCAC), which have been developed and used in restoration of underwater steel structures and salvage situation [4]. The FCAC method has much higher production efficiency than traditional dry or local dry underwater cutting because of the absence of complicated chamber, shielding gas or additional oxygen supply [5].

For self-shielded underwater wet cutting / welding, the key condition for the existence of arc is to generate vapor-gas bubble around the arc [6]. It appears as the wire touching approaching to the base metal, at the expense of heating from the contact area by transmitted current. After wire breaking off, the arc appears inside the bubble. The gas formed by the decomposition of flux inside the wire, the reaction between the base metal and wire, and the dissociation of water in the arc, cause the bubble to grow. The volume of bubble rises up to critical size owing to arc burning, then a part of bubble comes to the surface and a new bubble begins to form, as shown in Fig. 1. In order to investigate the continuous change of arc and gas bubble, Guo et al. [7] studied the droplet

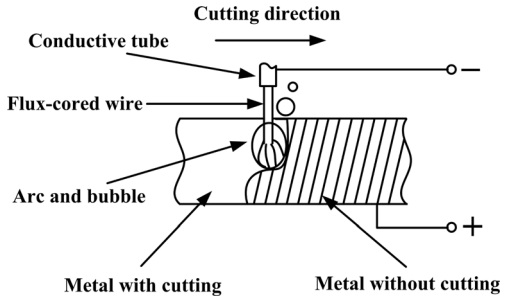

Fig. 1 Mechanism of the underwater flux-cored arc cutting

transfer process under underwater FCAW condition using the X-ray transmission method, Jia et al. [8] studied the spectroscopic analysis of the arc plasma of FCAW in air and underwater, Chen et al. [9] obtained electrical information of underwater FCAW to analyze the arc stability. In addition, the cooling times from 800 to 500 °C ($t_{8/5}$) is recommended as an important parameter which qualitatively analyzes the microstructure in HAZ. The $t_{8/5}$ is approximately 1 s during air-arc cutting process [10] while it is about 0.97 s under underwater welding condition [11], but studies on underwater wet FCAC are scarce.

The unique feature of underwater FCAC is the flux inside the wire, which usually consists of gas-forming agent, oxidant, and arc stabilizer. It is found that during underwater FCAC process, the base metal is melted by the heat of both the arc and the exothermic reaction in the oxygen environment, and blown off by airflow produced by the flux, while the arc is burning continuously between wire and base metal [12]. Although the continuous cutting can be obtained through optimizing the flux composition and adjusting the process parameters without additional oxygen supply, little information about the underwater cutting mechanism, e.g., temperature field, stress field and the microstructure has been reported, due to fluctuating of opaque vapor-gas bubbles around the arc. In particular, attention should be paid to the temperature field during cutting process owing to its important influence on the mechanical property and microstructure of the heat affected zone (HAZ) near the cut cavity, providing the basis for further processing of workpiece after cutting.

Due to the limits on experiment methods, finite element method (FEM) has been widely used to study the temperature field in welding & cutting. Hu et al. [10] developed a three-dimensional finite element model to study the material removal and the thermal effect of the arc on the temperature and stress fields of 10Ni5CrMoV steel plate during air-arc cutting process. Zhao et al. [13] focused on establishing the numerical model for analyzing the thermal process and the temperature field in underwater wet FCAW by means of FEM. Pan et al. [14] introduced the pool boiling heat transfer theory in numerical simulation of underwater welding process and proved to be applicable. Under underwater wet FCAC condition, the temperature gradient is much steeper owing to the existence of cut cavity and the notable effect of water environment on thermal cycle characteristics. In present study, the underwater wet cutting experiment was carried out using FCAC method, and the finite element model including the material removal and the thermal effect of the arc was developed to study the temperature field during underwater FCAC process. Developed FEM model was validated by comparing the distribution of temperature field obtained through experimental measurement and numerical computation. Moreover, HAZ was determined, which was very valuable for clarifying the mechanism of FCAC and adjusting the parameters of FCAC process.

Table 1 Parameters of underwater arc cutting

Voltage (V)	Current (A)	Torch height (mm)	Wire feeding speed (m/min)	Cutting speed (mm/min)	Water depth (mm)
40	350	8	4.5	130	150

2 Experiments

2.1 Flux-cored wire design and preparation

In present study, dolomite and cellulose were adopted as gas generator, while peroxide and its catalyzer were chosen to supply oxygen based on the previous work [15]. Moreover, gas producing components and elements with lower

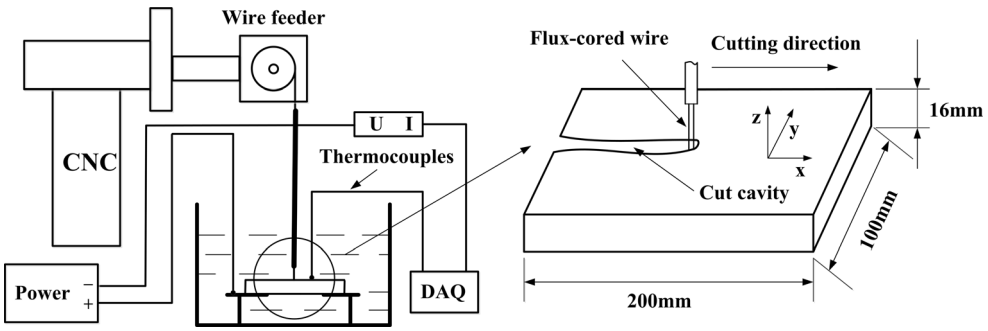

Fig. 2 Schematic diagram of the workpiece and the equipment of FCAC

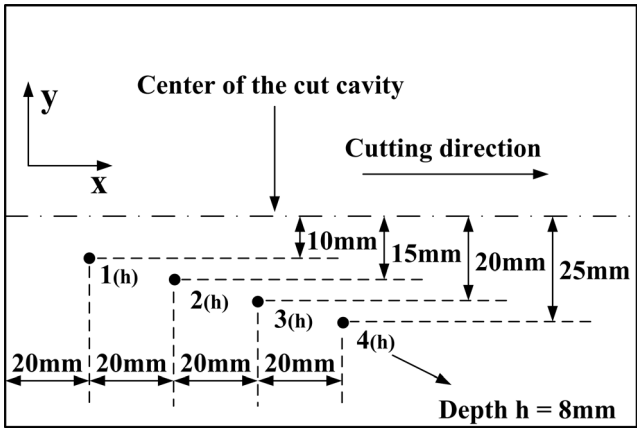

Fig. 3 Schematic diagram of the temperature measure position

ionization energy were added in the flux to improve the arc burning stability.

The cold rolling coil H08A steel with 8 mm width and 0.5 mm thickness was prepared. The steel strip was initially shaped into U-shape, and then closed as round-shaped after homogeneous flux powder mixture was wrapped within the U-shaped strip. The round-shaped steel strip was then drawn for multiple times, until the round-shaped steel strip became Φ2.2 mm diameter circular-shaped shell.

2.2 Underwater arc cutting with flux-cored wire

The gas metal arc welding (GMAW) machine with constant external characteristic was applied as the cutting power source, and the Q235 steel plate with the dimension of 200 mm × 100 mm × 16 mm was prepared as the experimental workpiece. As shown in Fig. 2, the x axis is the cutting direction, the y axis is the width direction, and the z axis is the thickness direction. The parameters of underwater arc cutting process in this study are listed in Table 1.

2.3 Temperature measure during underwater FCAC process

The thermocouples were welded to measure the thermal cycles of different points with all 8 mm depths from the workpiece surface and 10, 15, 20, 25 mm distances from the cut cavity center, as shown in Fig. 3, and then the data was recorded by data acquisition (DAQ). The K-type thermocouples were put in the 3.5 mm-diameter and 8 mm-depth holes drilled in the workpiece, and waterproof silicone was applied to prevent water into the hole, as shown in Fig. 4.

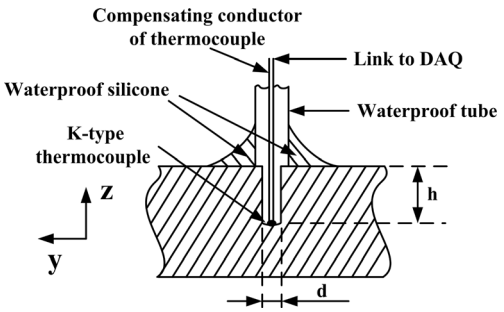

Fig. 4 Schematic diagram of the installation of the thermocouple

2.4 Analysis of the cutting process

During underwater FCAC process, the variation of the arc length or the wire extension has an effect on the shape of cut cavity. Firstly, the arc is generated between wire and base metal once the flux-cored wire touches the base metal. With the removal of molten base metal and the feeding of wire, the lateral surface of wire moves continuously nearer to edges of cut cavity. Then the arc burns between lateral surface of wire and cut cavity sidewall until the wire piece burns out. As the cutting torch moves forward, the new wire tip appears and the arc comes back to first space again. Accordingly, the arc repeatedly burns from "wire tip - molten metal" space to "wire lateral surface - cut cavity edge" space, then returns to the former space, and this cycle repeats periodically [5]. The top-view and cross-section images of the workpiece after cutting are shown in Fig. 5, and the width of cut cavity is about 8 ~ 11 mm. Owing to the entrance of wire to the cut cavity resulting in the arc burning between wire and cut cavity sidewall during underwater FCAC process, the lower part of cut cavity is relatively wider than the upper part [16].

During underwater FCAC process, there is no current at open circuit arc voltage, and there is a sharp decrease in arc voltage and corresponding increase in cutting current, as recorded in Fig. 6. It can also be observed from Fig. 6 that the variations of current and voltage during cutting period (without considering the arc striking and arc extinguishing periods) are relatively small; therefore the cutting process can be assumed to be a quasi-steady state with almost the constant heat input. The measured current and voltage in Fig. 6 are possible to support the above mechanism of FCAC process, which is also important for the finite element method.

3 Numerical simulation

3.1 Heat source model

Double-Ellipsoidal volumetric heat source model was selected to simulate the temperature field. The model is made up from two semi-ellipsoids, one at the front and one at the rear.

The power density distribution of the double-ellipsoidal heat source can be expressed by the following equations:

$$q_f(x,y,z) = \frac{6\sqrt{3}f_f Q}{\pi\sqrt{\pi}a_f bc}\exp\left\{-3\left[\left(\frac{x}{a_f}\right)^2+\left(\frac{y}{b}\right)^2+\left(\frac{z}{c}\right)^2\right]\right\} \quad (1)$$

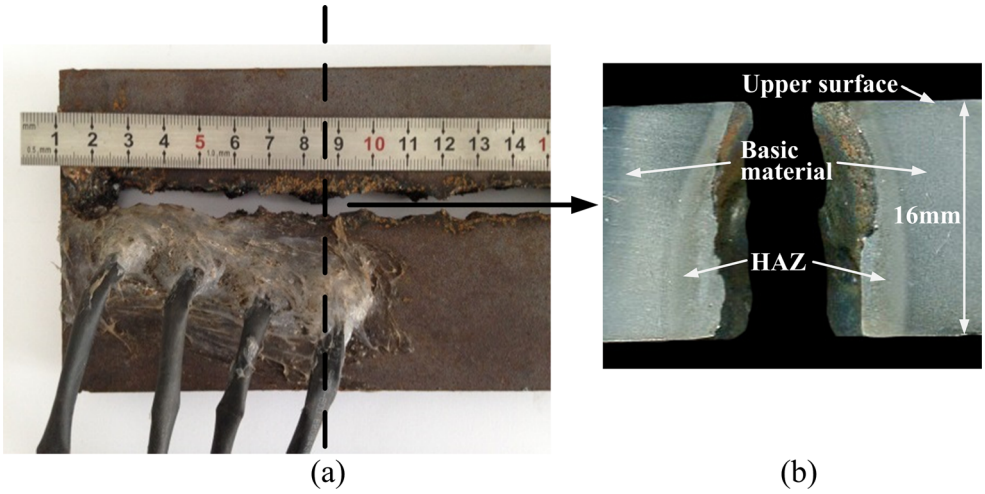

Fig. 5 Morphology of workpiece after cutting: **a** top view and **b** cross section

$$q_r(x,y,z)=\frac{6\sqrt{3}f_rQ}{\pi\sqrt{\pi}a_rbc}\exp\left\{-3\left[\left(\frac{x}{a_r}\right)^2+\left(\frac{y}{b}\right)^2+\left(\frac{z}{c}\right)^2\right]\right\} \quad (2)$$

$$f_f=\frac{2a_f}{a_f+a_r} \quad (3)$$

$$f_r=\frac{2a_r}{a_f+a_r} \quad (4)$$

$$f_f+f_r=2 \quad (5)$$

Where q_f and q_r are heat densities at spatial point (x, y, z) inside the front (f) and rear (r) half-ellipsoids; f_f and f_r are the fractional factors of the heat deposited in the front and rear hemispheres; x, y and z are the local coordinates of the double ellipsoid model aligned with the welded pipe; the parameters a_f, a_r, b and c are related to the characteristics of the cutting heat source; Q is the power of the cutting heat source. The values for different variables in the power density distribution equation are adjusted and optimized according to the profile of the cut cavity with large amounts of trial simulations, as given in Table 2.

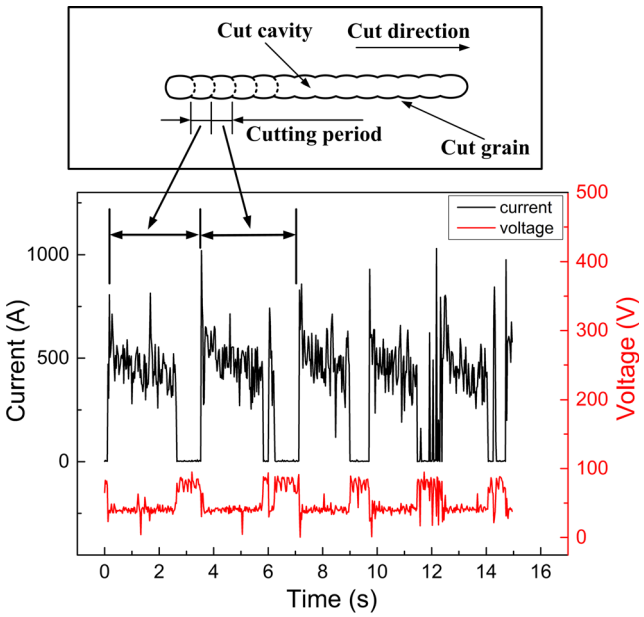

Fig. 6 Current and voltage during underwater FCAC process

The transient temperature field in the workpiece during underwater FCAC is influenced by two factors. The first one is the heat characteristic determined by arc thermal efficiency, and the second one is the heat characteristic determined by the thermal conductivity, workpiece thickness, cutting speed and water cooling effect. The heat source model is vital to numerical simulation analysis of cutting temperature field. During underwater FCAC process, the cutting heat comes from two parts, one is the arc heat, and the other is oxidation reaction heat.

The effective heat input Q is:

$$Q=\eta UI+Q_m \quad (6)$$

Where η is thermal coefficient; U is the average voltage during cutting period; I is the average current during cutting period; Q_m is the oxidation reaction heat.

Table 2 Double ellipsoid heat source parameters

Description	Symbol	Value
Front ellipsoidal semi-axes length	a_f	3 mm
Rear ellipsoidal semi-axes length	a_r	6 mm
Half width of arc	b	4 mm
Depth of arc	c	6 mm
Fraction of heat deposited in front	f_f	0.67
Fraction of heat deposited in rear	f_r	1.33
Arc efficiency	η	0.6

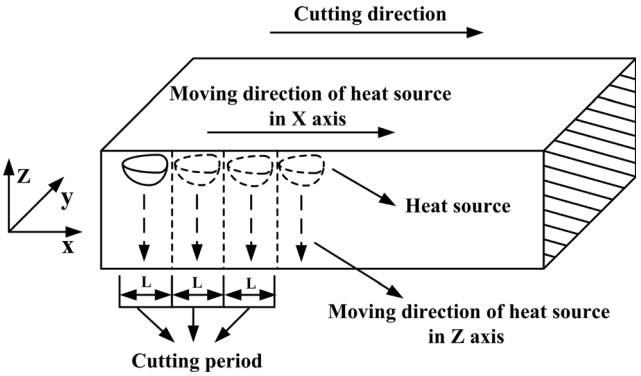

Fig. 7 Path of the heat source

There are three forms involved in the reaction of iron and oxygen, as following [17]:

$$Fe + 0.5O_2 \Rightarrow FeO + 267.8kJ \quad (7)$$

$$2Fe + 1.5O_2 \Rightarrow Fe_2O_3 + 823.2kJ \quad (8)$$

$$3Fe + 2O_2 \Rightarrow Fe_3O_4 + 1120.5kJ \quad (9)$$

The value of Q_m can be obtained according to the oxygen produced by the flux-cored and the above chemical equations. In the present study, Q_m is approximately 527 kJ, and the thermal efficiency of the underwater η is equal to 0.6.

The ANSYS software was used to simulate the moving of the heat source, as shown in Fig. 7. During simulation, the underwater metal arc cutting process is simplified as a cycle moving process of the heat source in z direction (thickness) and x direction (cutting direction). It means that the heat source moves along z direction first at the start location from the top surface to the bottom surface to simulate the cutting along depth, after the workpiece is cut through, the heat source moves forward in the x direction to a location (the distance is calculated by the cutting speed) on the top surface and then it moves along z direction again to achieve depth cutting. The action depth of the heat source is achieved by the movement of local coordinate systems programmed by the ANSYS parametric design language (APDL), i.e. when the heat source moves to a location on the top surface, a series of local coordinate systems are built with variation of z-coordinate to simulate the movement in depth, and the heat source model with the constant parameters is fixed on the local coordinate systems, thus the movement in depth of the heat source model is achieved without changing the parameters. In addition, the element death and birth technique was used to simulate the process that the melted metal was blown away from the workpiece.

3.2 Finite element model

To save the computation time, half of the workpiece was modeled due to the symmetry of the cutting process. Element meshes are denser in the vicinity of the cutting centerline, while the meshes become gradually coarser away from the cutting zone.

The finite model consists of 50,872 solid elements and 46,274 nodes. The finite element mesh is shown in Fig. 8.

3.3 Heat transfer boundary conditions

Assuming that the water in the sink did not flow and the bubbles rose freely during the experiment, meanwhile, the nearby water fills the cutting region and then vaporized. This process would not disappear until the temperature of cutting region fells below the boiling point. According to the pool boiling heat transfer theory [14, 18], the convective heat transfer coefficient h_c, which is the key factor to analyze the temperature field of underwater FCAC process, can be calculated by the following equations.

$$\begin{cases} h_c = 250, & T \le 100; \\ h_c = 250 + 353 \times (T-100), & 100 < T \le 130; \\ h_c = 10840-109 \times (T-130), & 130 < T \le 220; \\ h_c = 1030, & T > 220 \end{cases} \quad (10)$$

Where, T is the surface temperature of the workpiece.

The calculated temperature-dependent convective heat transfer coefficient by Eq.(10) is shown in Fig. 9. The convective boundary conditions are not only applied on the outer surface of the workpiece, but also on the two walls of the

Fig. 8 Finite element model

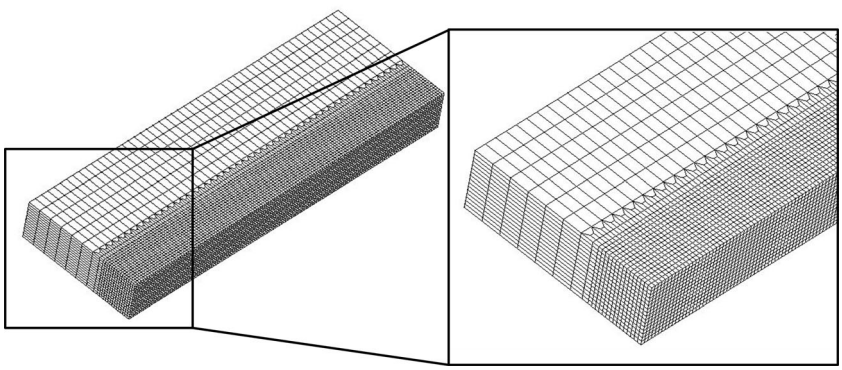

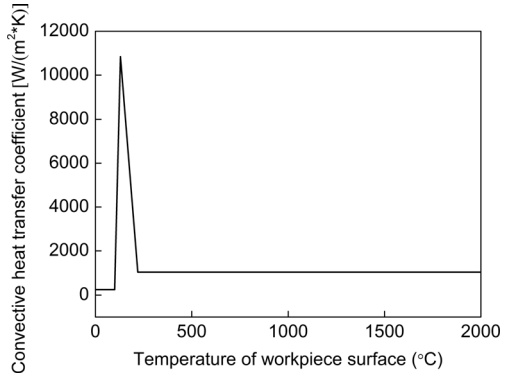

Fig. 9 Convective heat transfer coefficient h_c

cut cavity after cutting. Because of symmetry model used, the adiabatic boundary condition is applied on the symmetry plane of the finite element model.

3.4 Material properties and assumptions

The temperature-dependent thermal properties of the low-carbon steel are considered as shown in Table 3. During simulation, the uniform initial temperature (20 °C) of the workpiece is assumed and the latent heat of fusion is neglected. In addition, only the convection heat loss is taken into account and the radiation heat loss is ignored.

4 Results and discussion

The comparison of thermal cycles of points (10 mm, 15 mm, 20 mm, and 25 mm distances from the cut cavity center in Fig. 3) obtained by FEM with those by experiment is shown in Fig. 10. The trend of numerical temperature variation is basically consistent with the experimental results, and the maximum gap of the peak temperatures between the numerical and experimental results is less than 10 °C. The hysteresis of the strong gas flow, the interference of electrical signal and manual factors during the cutting process could cause the discrepancy. The fluctuations of the thermal cycles (circle parts in Fig. 10) are found at the locations close to the cut cavity, which are also found in experimental results by Hu et al. [10]. The peak temperature is caused by the nearest heating period from thermocouple, while the fluctuation is considered as a result of the combined effect of two or more heating periods during underwater FCAC process. The fluctuation is scarce if the thermocouple is not nearby the cut cavity, as the combined effect of heating periods is not obvious.

The temperature field of the workpiece in one cutting cycle is shown in Fig. 11. The maximum temperature exceeds 2873 °C, much higher than the melting point of the base metal in Fig. 11a. Then the molten pool moves continuously to the bottom of the workpiece, as shown in Fig. 11b~d. At the same time, the temperature on the cut cavity top decreases rapidly due to the strong cooling effect in water environment. Figure 11e shows the temperature field when the cutting has been completed, and the maximum temperature decreases below the melting point of the base metal as soon as the arc disappears.

The thermal cycles of No.1 ~ 25 points (x = 40 mm) near the cut cavity (as shown in Fig. 12a) were calculated, which were shown in Fig. 12b~f, and the calculated peak temperatures of these points were shown in Fig. 13.

The calculated peak temperatures of points on the workpiece upper surface with 5, 6, 7, 8, 10 mm distances from the cut cavity center (No. 1 ~ 5) are around 835 °C, 374 °C, 254 °C, 238 °C, and 164 °C, while those of points No. 21 ~ 25 are around 1670 °C, 1340 °C, 777 °C, 441 °C, and 234 °C, respectively. The calculated peak temperature of No. 21 is 1670 °C, which means that this point is melted and blown off. The calculated peak temperature of point (x = 40 mm, y = 4 mm, z = 16 mm) is over 2000 °C, which is not plotted in the result.

When the value of z is constant, the temperature of point is decreased with the increase of the distance from the cut cavity center. During underwater FCAC process, after the upper part of workpiece is separated from the base material, the considerable heat is transferred from the heat source to the cut cavity and the lower part of the workpiece. Thus under the same distance from the cut cavity center condition, the temperature of point is increased with the increase of depth.

The $t_{8/5}$ values of points (No.1, 6, 11, 12, 16, 17, 21, and 22 in Fig. 12) whose peak temperatures are above 800 °C are shown in Fig. 14. The calculated $t_{8/5}$ value is shorter than 0.5 s, which is much shorter than the one of air-arc cutting process (approximately 1 s [10]) due to the strong cooling effect of water. The calculated $t_{8/5}$ value of No.12 is only 0.38 s, that is to say, the average cooling speed from 800 to 500 °C is close to 800 °C/s. During underwater FCAC process, the larger input power leads to the base metal under the electric

Table 3 Thermo-mechanical material properties of Q235

Temperature (°C)	20	250	500	750	1000	1500	1700	2500
Thermal conductivity λ (W/m·°C)	50	47	40	27	30	35	140	142
Density ρ (kg/m^3)	7820	7700	7610	7550	7490	7350	7300	7090
Specific heat c [J/(kg·°C)]	460	480	530	675	670	660	780	820

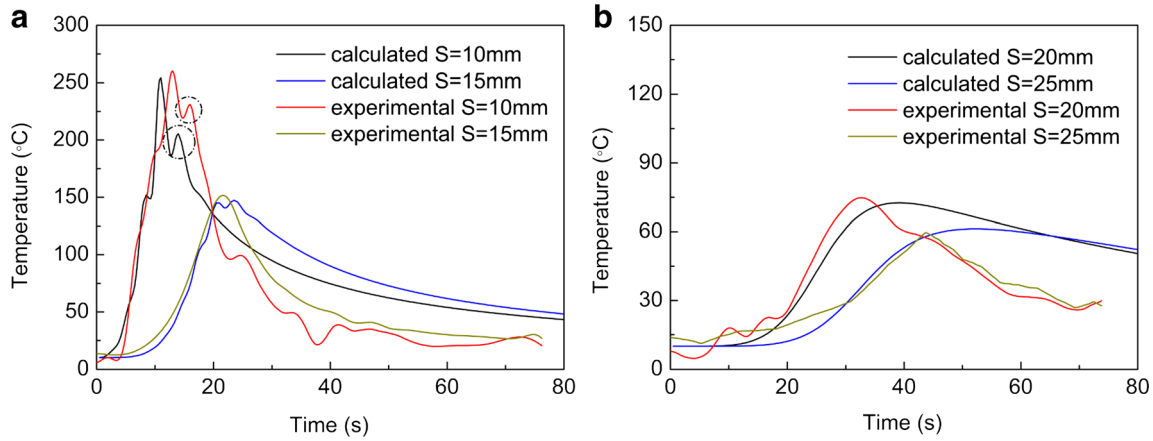

Fig. 10 Comparison of calculated and experimental thermal cycles during underwater FCAC process: **a** 10 mm, 15 mm distances from the cut cavity center and **b** 20 mm, 25 mm distances from the cut cavity center

arc beam reaching the melting point instantly, and the considerable heat loss results in the faster cooling with the removal of molten base metal, while the cooling rate is relatively lower due to droplet transfer under underwater welding condition (the $t_{8/5}$ is about 0.97 s, and the cooling rate is approximately 310 °C/s as reported [11]).

In this study, calculated result of HAZ (the temperature to decide the HAZ is higher than 800 °C) is shown in Fig. 15, and the experimental HAZ as shown in Fig. 5 is also plotted in Fig. 15. As mentioned in Fig. 5b, the width of cut cavity is about 8 ~ 11 mm in this study, and the lower part of cut cavity is relatively wider than the upper part. During underwater FCAC process, the heat transfers from the upper part of workpiece to lower part, and the base metal in upper part is removed earlier than that in lower part. Therefore, the width of HAZ near lower part of the cut cavity (about 3 ~ 4 mm) is relatively larger than that near upper part (about 1 ~ 2 mm), from the experimental results of HAZ.

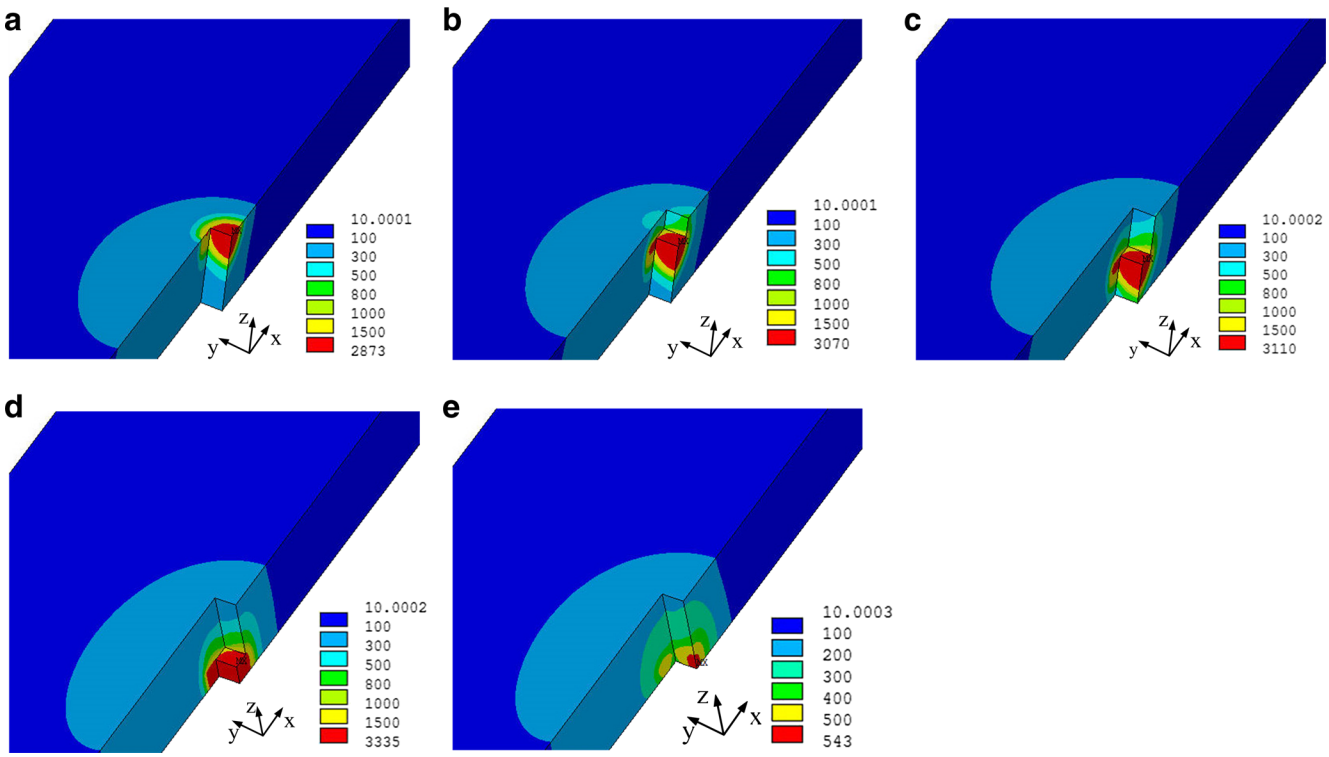

Fig. 11 Temperature field of the workpiece in one cutting cycle at **a** t = 30.5 s, **b** t = 31 s, **c** t = 31.5 s, **d** t = 32 s, and **e** t = 33 s

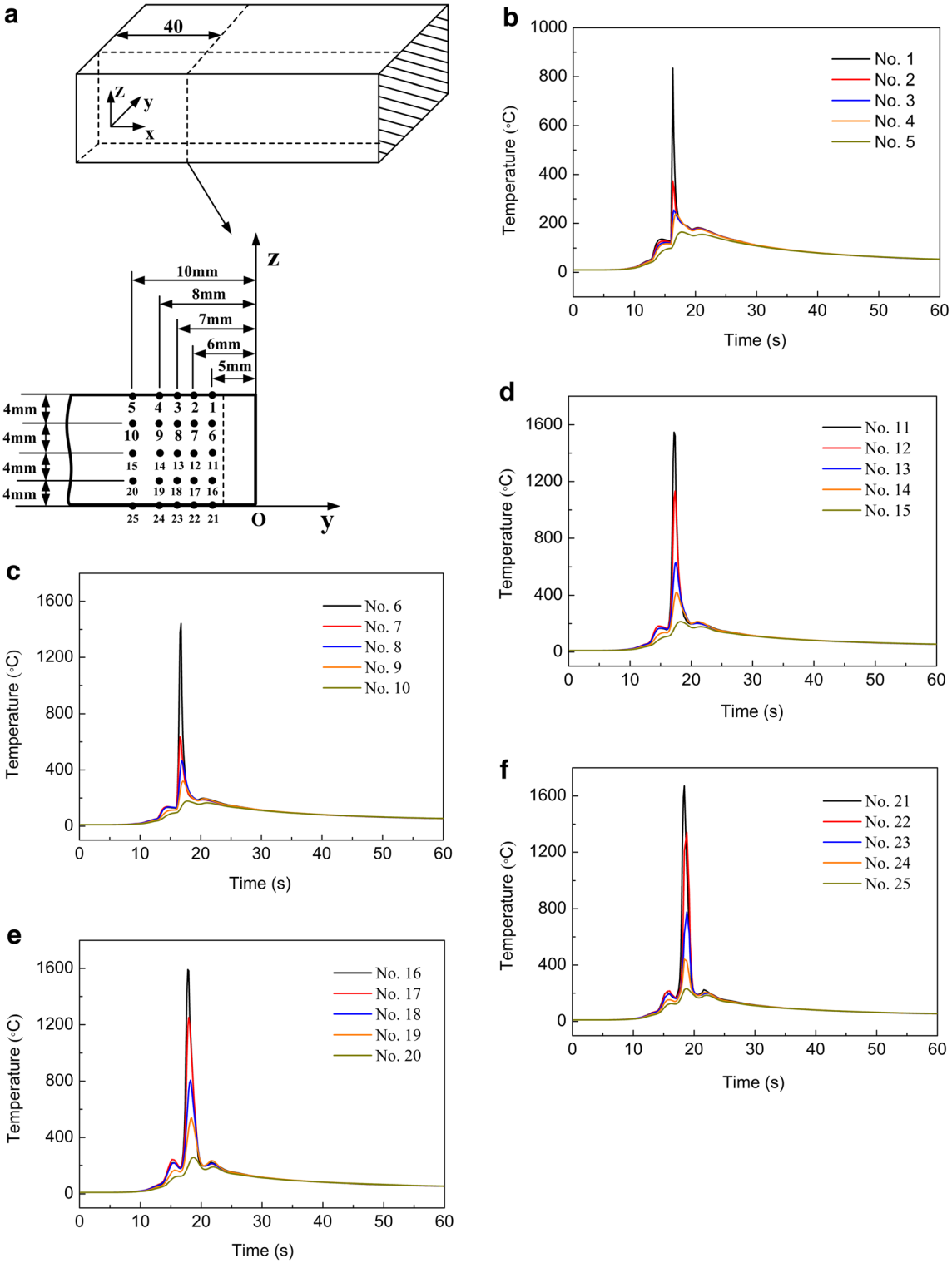

Fig. 12 Calculated thermal cycles of different points (x = 40 mm) during underwater FCAC process: **a** the location of different points, **b** No.1 ~ 5, **c** No.6 ~ 10, **d** No.11 ~ 15, **e** No.16 ~ 20, and **f** No.21 ~ 25

In general, the results of FEM agree well with experimental results. Temperature distributions obtained by both FEM and experiments provide a useful data base for further research on underwater FCAC mechanism, as well as cutting process automation. Undergoing work is being conducted to further improve the accuracy of experiment and numerical calculation, under shallow water and deep water condition.

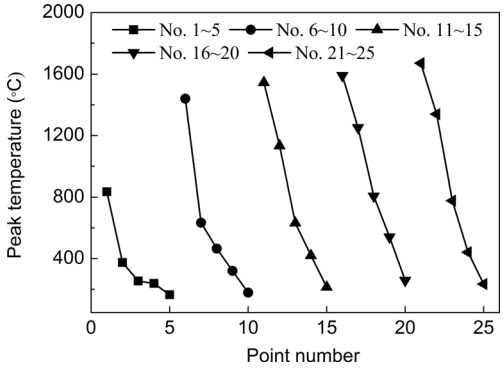

Fig. 13 Calculated peak temperatures of points in Fig.12

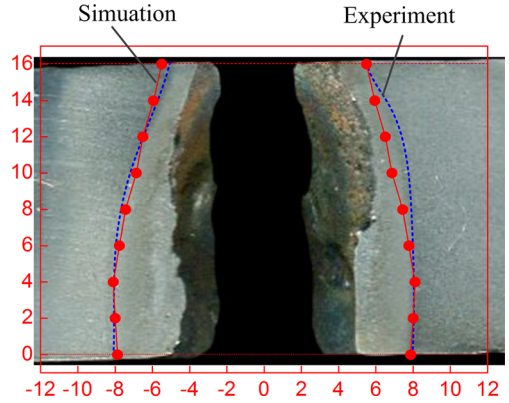

Fig. 15 Calculated and experimental results of HAZ

5 Conclusions

The underwater cutting experiment was conducted using flux-cored wire cutting method, and temperature distribution was measured using thermocouples. Subsequently, the temperature field was simulated by means of finite element method. The conclusions can be summarized as follows:

(1) According to the mechanism of underwater FCAC, double ellipsoid heat source model considering arc heat as well as chemical heat was introduced, and the boundary condition of pool boiling heat transfer was selected. The calculated thermal cycles during underwater FCAC process match well with those acquired by the experiment, which proves the model and boundary condition in this study to be applicable for underwater FCAC.

(2) The characteristics of the temperature field of underwater FCAC are obtained, and the calculated $t_{8/5}$ value is shorter than 0.5 s, which is much shorter than the one of air-arc cutting process and the one of underwater welding process.

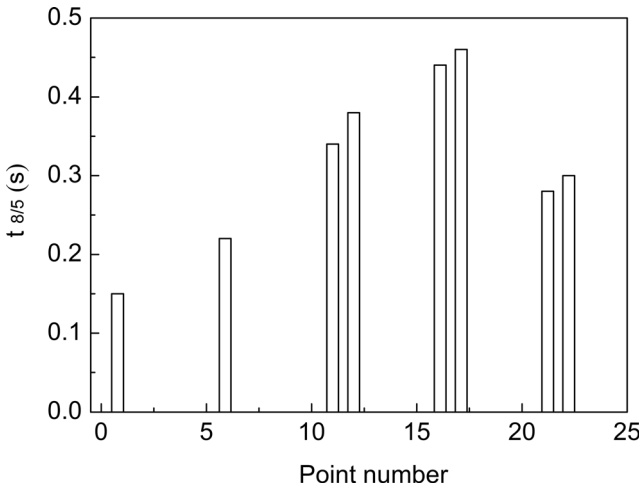

Fig. 14 Calculated cooling times from 800 to 500 °C of some points in Fig.12

(3) The width of cut cavity is about 8 ~ 11 mm in this study, and the lower part of cut cavity is relatively wider than the upper part, owing to the entrance of wire to the cut cavity resulting in the arc burning between wire and cut cavity sidewall during underwater FCAC process.

(4) The width of HAZ near lower part of the cut cavity (about 3 ~ 4 mm) is relatively larger than that near upper part (about 1 ~ 2 mm).

Acknowledgements This work was carried out with the support of National Natural Science Foundation of China (51305173), China Postdoctoral Science Foundation (General Financial Grant 2014 M550289, 2015 M580423, and Special Financial Grant 2015 T80548, 2016 T90453), and a Project Funded by the Priority Academic Program Development of Jiangsu Higher Education Institutions.

References

1. Bach FW, Bienia H, Versemann R, Philipp E (2002) High-performance thermal cutting techniques for underwater use. ATW Internationale Zeitschrift fuer Kernenergie 47:250–252
2. Frazer I, Fyffe L, Gibson OJ, Lucas B (2002) Remotely operated underwater thermal cutting processes for the decommissioning of large North Sea platforms. In: Proceedings of OMAE'02 21st International Conference on Offshore Mechanics and Arctic Engineering, American Society of Mechanical Engineers, Oslo, Norway, pp 535–542
3. Steiner H (2012) Dismantling and demolition processes and technologies in nuclear decommissioning projects. In: nuclear decommissioning. Woodhead Publishing, Cambridge, pp 293–318
4. Kononenko VY (2014) Underwater welding and cutting in CIS countries. Paton Welding Journal (6–7): 40–45
5. Gretskii YY, Nefedov YN (1998) Study of peculiarities of underwater flux-cored wire arc cutting without additional supply of oxygen. In: underwater wet welding and cutting. Woodhead Publishing, Cambridge, pp 87–95
6. Yushchenko KA, Gretskii YY, Maksimov SY (1998) Study of physico-metallurgical peculiarities of wet arc welding of structural steels, in: underwater wet welding and cutting. Woodhead Publishing, Cambridge, pp 6–29

7. Guo N, Du YP, Feng JC, Guo W, Deng Z (2015) Study of underwater wet welding stability using an X-ray transmission method. J Mater Process Technol 225:133–138
8. Jia CB, Zhang T, Maksimov SY, Yuan X (2013) Spectroscopic analysis of the arc plasma of underwater wet flux-cored arc welding. J Mater Process Technol 213:1370–1377
9. Chen B, Tan C, Feng J (2015) A study on the arc characteristics of underwater wet welding process. Int J Adv Manuf Technol 86:557–564
10. Hu JF, Yang JG, Fang HY, Li GM, Zhang Y, Wan X (2007) Temperature stress and microstructure in 10Ni5CrMoV steel plate during air-arc cutting process. Comp Mater Sci 38:631–641
11. Mei FX, Yu SZ (1982) Translation essays in underwater welding and cutting. China Machine Press, Beijing (in Chinese)
12. Nefedov YN, Danchenko ME (1998) Technology and experience of application of underwater flux-cored wire arc semi-automatic cutting. In: underwater wet welding and cutting. Woodhead Publishing, Cambridge, pp 96–104
13. Zhao B, Wu CS, Jia CB, Yuan X (2013) Numerical analysis of the weld bead profiles in underwater wet flux-cored arc welding. Acta Metall Sin 49:797–803
14. Pan J, Yang L, Hu S, Chai S (2016) Numerical analysis of thermal cycle characteristics and prediction of microstructure in multi-pass UWW. Int J Adv Manuf Technol 84:1095–1102
15. Wang JX, Wang JY, Li WH, Zhu J (2012) A kind of flux-cored cutting wire for underwater wet arc cutting and its preparation. CN201210057823.9 (in Chinese)
16. Li WH, Wang W, Wang JX, Yang F, Zhu J, Wang JY (2012) Research on the underwater arc cutting method of flux-cored wire. Journal of Shanghai Jiaotong University 46:117–119 (in Chinese)
17. Liang GF (1997) Cutting technology manual. China Machine Press, Beijing (in Chinese)
18. Li H (2012) Temperature field simulation and metallurgical analysis of underwater wet welding process. Dissertation, Tianjin University (in Chinese)